Factors Determining Electron-Transfer Rates in Cytochrome *c* Oxidase: Studies of the FQ(I-391) Mutant of the *Rhodobacter sphaeroides* Enzyme†

Pia Ädelroth,‡ David M. Mitchell,§ Robert B. Gennis,§ and Peter Brzezinski*,‡

Department of Biochemistry and Biophysics, University of Göteborg and Chalmers University of Technology, Medicinaregatan 9C, S-413 90 Göteborg, Sweden, and School of Chemical Sciences, University of Illinois, Urbana, Illinois 61801

Received November 14, 1996; Revised Manuscript Received July 9, 1997⊗

ABSTRACT: The mechanisms of internal electron transfer and oxygen reduction were investigated in cytochrome *c* oxidase from *Rhodobacter sphaeroides* (cytochrome aa_3) using site-directed mutagenesis in combination with time-resolved optical absorption spectroscopy. Electron-transfer reactions in the absence of O_2 were studied after flash photolysis of CO from the partly-reduced enzyme and the reaction of the fully-reduced enzyme with O_2 was studied using the so-called flow−flash technique. Results from studies of the wild-type and mutant enzyme in which phenylalanine-391 of subunit I was replaced by glutamine (FQ(I-391)) were compared. The turnover activity of the mutant enzyme was ∼2% (∼30 s^{-1}) of that of the wild-type enzyme. After flash photolysis of CO from the partly-reduced mutant enzyme ∼80% of Cu_A was reduced, which is a much larger fraction than in the wild-type enzyme, and the rate of this electron transfer was 3.2×10^3 s^{-1}, which is significantly slower than in the wild-type enzyme. The redox potentials of hemes *a* and a_3 in the mutant enzyme were found to be shifted by about +30 and −70 mV, respectively, as compared to the wild-type enzyme. During the reaction of the fully-reduced FQ(I-391) mutant enzyme with O_2 a rapid kinetic phase with a rate constant of 1.2×10^5 s^{-1}, presumably associated with O_2 binding, was followed by formation of the P intermediate with electrons from heme a_3 and Cu_B with a rate of $\sim 4 \times 10^3$ s^{-1}, and oxidation of the enzyme with a rate of ∼30 s^{-1}. The dramatically slower electron transfer between the hemes during O_2 reduction in the mutant enzyme is not only due to the slower intrinsic electron transfer, but also due to the altered redox potentials. In addition, the results show that the reduced overall activity of the mutant enzyme is due to the slower electron transfer from heme *a* to the binuclear center during O_2 reduction. The relation between the intrinsic heme *a*/heme a_3 electron-transfer rate and equilibrium constant, and the electron-transfer rate from heme *a* to the binuclear center during O_2 reduction is discussed.

During the catalytic cycle of cytochrome *c* oxidase, electrons from cytochrome *c* are first transferred to copper A (Cu_A),[1] followed by transfer to heme *a* and then to the binuclear center, consisting of copper B (Cu_B) and heme a_3. The enzyme from *Rhodobacter sphaeroides* is structurally and functionally very similar to the mitochondrial enzyme (Hosler et al., 1992; Calhoun et al., 1994) but is composed only of three protein subunits instead of 13. Recently, the structures of both the bovine (Tsukihara et al., 1995, 1996) and *Paracoccus denitrificans* (Iwata et al., 1995) cytochrome *c* oxidases were determined to atomic resolution [for a recent review on structure and function of cytochrome *c* oxidase see Ferguson-Miller and Babcock (1996)].

To elucidate the mechanisms of electron and proton transfer in cytochrome *c* oxidase these reactions have earlier been studied in different states of the enzyme using various spectroscopic techniques. For example, rapid internal electron-transfer reactions in the absence of O_2 have been studied in the partly reduced enzyme after flash photolysis of carbon monoxide bound to the binuclear center (Boelens et al., 1982; Brzezinski & Malmström, 1987; Ädelroth et al., 1995, 1996). In the two-electron reduced (mixed valence) CO-bound enzyme the electrons are found at heme a_3/Cu_B. After CO dissociation in the *R. sphaeroides* enzyme there is a fractional electron transfer from heme a_3 to heme *a* with an observed rate constant of 3.7×10^5 s^{-1} followed by slower equilibration with Cu_A with a rate constant of 2.8×10^4 s^{-1} (Ädelroth et al., 1995). In the three-electron reduced CO-bound bovine enzyme the additional electron is mainly found at heme *a* and after CO photolysis it equilibrates with Cu_A with a rate constant of about $\sim 2 \times 10^4$ s^{-1} (Morgan et al., 1989).

The reaction of the fully-reduced enzyme with dioxygen has been studied using the so-called flow−flash technique (Gibson & Greenwood, 1963). Fully reduced CO−cytochrome *c* oxidase is mixed rapidly with a dioxygen-containing buffer. Pulsed illumination a short time after mixing results in dissociation of CO which allows the reduced enzyme to react with O_2. The flow−flash technique, combined with different spectroscopic techniques, has provided information about the intermediate steps during O_2 reduction [reviewed in Babcock and Wikström (1992), Babcock and Varotsis (1993), Ferguson-Miller and Babcock

† Supported by grants to P.B. from the Swedish Natural Science Research Council, Carl Trygger's Foundation, and The Magne Bergvall Foundation and to R.B.G. from the National Institutes of Health.

* Address correspondence to this author. FAX: +46 31 773 3910. E-mail: peter@bcbp.gu.se.

‡ University of Göteborg and Chalmers University of Technology.

§ University of Illinios.

⊗ Abstract published in *Advance ACS Abstracts,* September 1, 1997.

[1] Abbreviations: Cu_A, copper A; Cu_B, copper B; A, ferrous-oxy intermediate; R, fully-reduced enzyme; O, fully-oxidized enzyme; P, peroxy intermediate ($P(Fe_a^{3+})$ and $P(Fe_a^{2+})$ when formed with electrons from hemes a/a_3, and heme a_3/Cu_B, respectively); F, ferryl intermediate. Nomenclature of the mutant enzymes: for example, replacement of phenylalanine-391 of subunit I with glutamine is denoted FQ(I-391); WT, wild type.

S0006-2960(96)02824-3 CCC: $14.00

(1996)]. For example, when used in combination with time-resolved optical absorption spectroscopy, at 445 nm, four kinetic phases are observed in the mitochondrial enzyme. First, O_2 binds to reduced heme a_3 with an observed rate of about 10^5 s^{-1} at 1 mM O_2 (Oliveberg et al., 1989; Verkhovsky et al., 1994; Sucheta et al., 1997), forming the ferrous−oxy intermediate (Varotsis et al., 1989; Han et al., 1990a; Ogura et al., 1990). It is followed by electron transfer from heme *a* to the binuclear center and formation of the peroxy intermediate (P) with a rate constant of 3×10^4 s^{-1} (Hill & Greenwood, 1984; Oliveberg et al., 1989; Han et al., 1990b; Morgan et al., 1996) leaving Cu_B reduced. The same P intermediate is also formed when the two-electron reduced enzyme (heme a/Cu_A oxidized and the binuclear center reduced, mixed-valence) reacts with O_2 (Morgan et al., 1996). At room temperature the rate constant for P formation from the mixed-valence state is $(5-6) \times 10^3$ s^{-1} (Hill & Greenwood, 1983; Oliveberg et al., 1989; Han et al., 1990b). In the fully-reduced enzyme, the ferryl intermediate (F) is formed and the electron at Cu_A equilibrates with heme *a* with a rate of about 1×10^4 s^{-1} (Hill & Greenwood, 1984; Hill, 1991; Morgan et al., 1996). The Cu_A-to-heme *a* electron transfer is most likely gated by proton uptake associated with the P → F transition (Hallén & Nilsson, 1992; Hallén & Brzezinski, 1994; Svensson Ek & Brzezinski, 1997). Finally, the electron at heme a/Cu_A is transferred to the binuclear center with a rate of about 600 s^{-1}, yielding the fully-oxidized enzyme (O) (Hill & Greenwood, 1984; Oliveberg et al., 1989; Hill, 1991).

The studies described above have shown that different rates of internal electron transfer are observed in different states of the enzyme. For example, the apparent electron-transfer rate between hemes *a* and a_3 varies by several orders of magnitude in different states of the enzyme ranging from ≤ 100 s^{-1} when reducing the oxidized enzyme (Antalis & Palmer, 1982; Sarti et al., 1990) to $\sim 10^5$ s^{-1} in the mixed-valence enzyme (Oliveberg & Malmström, 1991; Ädelroth et al., 1995). During dioxygen reduction, the transfers of the third and fourth electrons to the binuclear center from heme *a* differ in rate by a factor of ~40, which shows that different mechanisms control these rates.

In order to understand the overall mechanism by which electron- and proton-transfer reactions are coupled during the catalytic cycle of cytochrome *c* oxidase it is important to understand factors that control rates of these reactions in different states of the enzyme. Therefore, in this study we have investigated a mutant of *R. sphaeroides* cytochrome *c* oxidase in which phenlylalanine I-391, a highly conserved residue, was replaced by glutamine (FQ(I-391)). In this mutant oxidase redox potentials and rates of internal electron-transfer reactions are altered. The aim of the present study is not to understand the role of F(I-391) but to use the FQ-(I-391) mutant enzyme as a tool to investigate the relation between electron-transfer rates in different states of the enzyme.

The overall turnover activity of the FQ(I-391) mutant oxidase was about 2% of that in the wild-type enzyme. In the FQ(I-391) mutant oxidase a dramatic effect on internal electron transfer in the partly-reduced state was observed. Following CO dissociation only one kinetic phase was observed, consistent with about 80% electron transfer from heme a_3 to Cu_A with a rate of 3.2×10^3 s^{-1}, indicating a shift of the heme a/a_3 equilibrium towards heme *a*.

Table 1: Rate Constants and Extents of Electron Transfer for Partly- and Fully-Reduced Wild-Type and FQ(I-391) Mutant Enzyme

	wild type		FQ(I-391)	
	rate (s^{-1})	extent (%)	rate (s^{-1})	extent
turnover (at pH 6.5)	1500	−	30	−
partly reduced $a_3 \rightarrow a$	2×10^5	40[a]	−	−
partly reduced $a_3/a \rightarrow Cu_A$	2.8×10^4	10[a]	3.2×10^3	80
flow flash, O_2 binding	4×10^4 [b]	65[c]	1.2×10^5	40[c]
flow flash, formation of P			4×10^3	5−10[c]
flow flash, oxidation	6×10^2	35[c]	30	50−55[c]

[a] Partly reduced wild-type and FQ(I-391) enzymes are two- and three-electron reduced, respectively. [b] This phase contains contributions of both O_2 binding ($\sim 10^5$ s^{-1}) and P-intermediate formation. [c] Fraction of the total (reduced−oxidized) absorbance change at 445 nm.

The reaction of the fully-reduced FQ(I-391) mutant enzyme with O_2 was initially similar to that observed in the mixed-valence (bovine) enzyme; a rapid change in absorbance ($k \cong 1.2 \times 10^5$ s^{-1}) associated with O_2 binding was followed by a slower change ($k \cong 4 \pm 2 \times 10^3$ s^{-1}), presumably associated with oxidation of heme a_3/Cu_B forming the peroxy intermediate. Electron transfer from heme *a* was much slower than in the wild-type enzyme, and the enzyme was oxidized with a rate of 30 s^{-1}. This shows that the smaller overall activity of the mutant enzyme is due to a slower electron transfer from heme *a* to the binuclear center during O_2 reduction, which is directly related to the shift of the heme a/a_3 equilibrium constant.

MATERIALS AND METHODS

Enzyme Preparation. The enzyme was prepared as described (Mitchell & Gennis, 1995), and the stock solution was stored in liquid nitrogen until used. The turnover activity of the FQ(I-391) enzyme was measured as described (Mitchell & Gennis, 1995) and was found to be about 2% of that of the wild-type enzyme (see Table 1). The UV−visible absorbance spectra of the oxidized, fully-reduced, and fully-reduced−CO FQ(I-391) enzyme were about the same as those of the wild-type enzyme, and the binuclear center was intact (Mitchell, 1996). Mutagenesis was performed as described (Mitchell, 1996).

Potentiometric Titration. The potentiometric titration of heme *a* was carried out in the presence of KCN which binds to the binuclear center and locks it in the oxidized state [at a saturating concentration of 4 mM for both the wild-type and FQ(I-391) mutant enzymes]. Heme *a* was first oxidized using potassium ferricyanide at a concentration of 50 μM. It was then gradually reduced by additions of aliquots of potassium ferrocyanide. Finally, the fully reduced state was attained by addition of an excess of dithionite. An E_m value of 430 mV was used for the ferrocyanide/ferricyanide couple. The procedure was performed aerobically in an open cuvette. The fraction reduced heme *a* was determined from absorbance changes in the α band, relative to the fully reduced state. After each addition of ferrocyanide, about 5 min was allowed for equilibration.

Preparation of Partly-Reduced Enzyme. The partly reduced enzyme was prepared as described previously (Brzezinski & Malmström, 1985). Briefly, the oxidized enzyme was diluted in 0.1 M Hepes-KOH (pH 7.0) and 0.1% dodecyl β-D-maltoside to a concentration of ~5 μM in a cuvette,

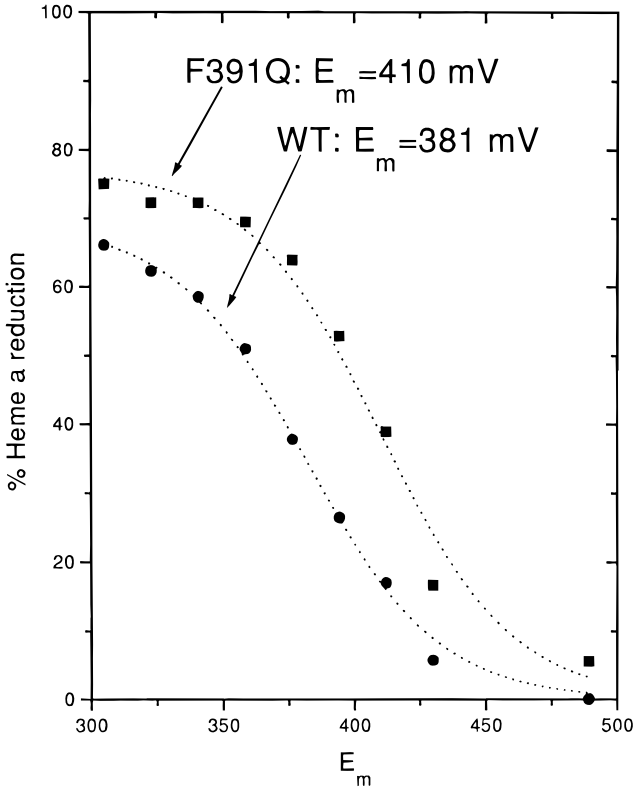

FIGURE 1: Redox titration of heme *a* with ferri/ferrocyanide. The initial concentration of potassium ferricyanide was 50 μM, after which aliquots of potassium ferrocyanide were added to alter the potential to a maximum ratio of ~100 (ferrocyanide/ferricyanide). Reduction levels of heme *a* at each step of the titration were determined from the absorbance spectrum in the α region. The enzyme concentration was ~2 μM. Buffer conditions were as follows: 100 mM Tris, pH 7.5, 0.1% dodecyl β-D-maltoside, 0.1 mM EDTA, 10 μg/mL polylysine, 4 mM KCN. The titrations were carried out at 25° C.

which was then evacuated on a vacuum line and flushed with CO at 1×10^5 Pa (~1 mM concentration). The enzyme was progressively reduced during CO incubation, and the 2−3-electron reduced state was formed after 0.5−5 h incubation time (see Results).

Preparation of Fully-Reduced Enzyme for Flow-Flash Experiments. The enzyme stock was diluted as described above but to a concentration of ~10 μM. It was first incubated under N_2 atmosphere for about 10 h in 2 mM sodium ascorbate as a reducing agent and 5 μM phenazine methosulfate as a mediator. After formation of the fully-reduced enzyme, N_2 was replaced with CO at 1×10^5 Pa.

Flow−Flash Experiments and Data Analysis. The enzyme solution was mixed with an O_2-saturated buffer in a locally modified stopped-flow apparatus (Applied Photophysics) at a ratio of 1:5. After mixing, the enzyme and O_2 concentrations were ~2 μM and ~1 mM, respectively. About 100 ms after mixing, CO was flashed off with a 10 ns, ~100 mJ laser flash at 532 nm (Nd:YAG laser from Spectra Physics) and the reaction between the fully-reduced enzyme and O_2 was followed at various wavelengths. The cuvette path length was 1.00 cm. Typically, 60 000 data points were collected and the data set was then reduced to 500−1000 points by averaging over a progressively increasing number of points (logarithmic time scale). Rate constants were determined using a nonlinear fitting algorithm on a personal computer.

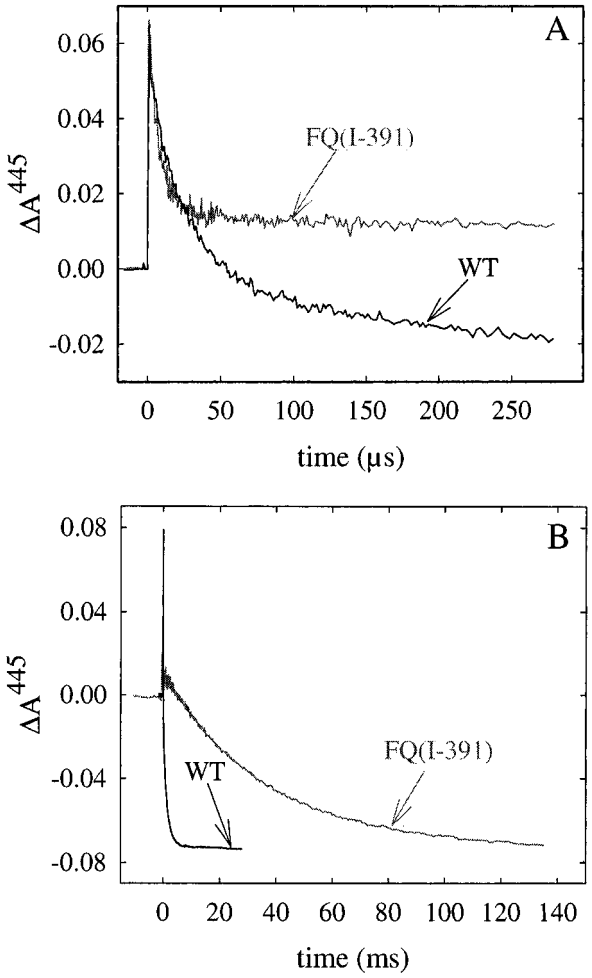

FIGURE 2: Absorbance changes at 445 nm associated with the reaction of the fully-reduced wild-type and FQ(I-391) mutant enzymes with O_2. The CO fully-reduced enzyme was mixed rapidly (in ~1 ms) with an O_2-containing buffer. About 100 ms after mixing, CO was flashed off (at $t = 0$). Note the different time scales in panels A and B. Conditions after mixing: 1 μM reacting cytochrome *c* oxidase, 100 mM Hepes, pH 7.4, 0.1% dodecyl β-D-maltoside, $[O_2] \cong 1$ mM.

RESULTS

Potentiometric Titrations. The redox potential of heme *a* was found to be 410 mV in the FQ(I-391) mutant enzyme, i.e., about 30 mV higher than in the wild-type enzyme (Figure 1).

Reaction of the Fully-Reduced Enzyme with O_2. Figure 2AB shows absorbance changes at 445 nm after flash photolysis of CO from the fully reduced cytochrome *c* oxidase−CO complex in the presence of dioxygen. The rapid increase in absorbance at the flash is associated with dissociation of CO. In the FQ(I-391) mutant enzyme it is followed by a decrease in absorbance with a rate of 1.2×10^5 s^{-1}. The kinetic difference spectrum of this phase (Figure 3A) is consistent with that of O_2 binding to heme a_3 (formation of the A intermediate) (Verkhovsky et al., 1994). The absorbance then decreases further with a rate of $(4 \pm 2) \times 10^3$ s^{-1} and an amplitude at 445 nm of about 10% of the first phase. This decrease is presumably associated with oxidation of heme a_3/Cu_B forming the peroxy intermediate, similarly to what is observed in the mixed-valence bovine enzyme (see introduction). It is followed by a much slower further decrease in absorbance with a rate of about 30 s^{-1} associated with full oxidation of the enzyme (Figure 2B). In

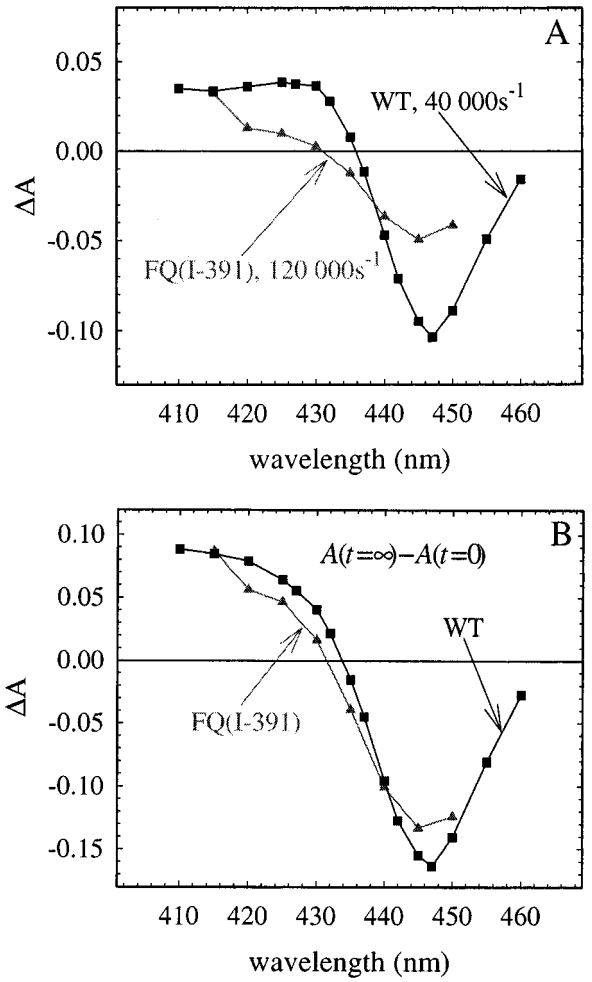

FIGURE 3: (A) Kinetic difference spectra of the 1.2×10^5 s^{-1} phase in the FQ(I-391) mutant (▲) and the 4×10^4 s^{-1} in the wild-type enzyme (■). (B) Kinetic difference spectra of the FQ(I-391) mutant (▲) and wild-type enzymes (■) calculated from the difference in absorbance at the end of the reaction ($A(t=\infty)$ and immediately after CO dissociation ($A(t=0)$). Conditions were the same as in Figure 2.

the wild-type enzyme three major kinetic phases were observed in the Soret region with rate constants of 4×10^4, 8×10^3, and 6×10^2 s^{-1}, respectively (Figure 2AB). In the α region a kinetic phase associated with O_2 binding with a rate constant of 1.2×10^5 s^{-1} was also observed (not shown). Thus the first phase in the Soret region most likely contains contributions both from O_2 binding to heme a_3 (formation of the A intermediate) and oxidation of hemes *a* and a_3 forming the P intermediate. The kinetic difference spectrum of this phase is shown in Figure 3A. The second and third phases are presumably associated with the peroxy-to-ferryl and ferryl-to-oxidized transitions, respectively (see introduction).

The concentration of active enzyme was calculated from the CO dissociation absorbance change. The absorbance immediately after the flash corresponds to the fully reduced enzyme whereas the absorbance at "infinite time", i.e. after completition of the reaction corresponds to the fully oxidized enzyme. A kinetic difference spectrum obtained from a difference of the absorbances at "infinite time" and immediately after the flash is shown in Figure 3B; they show that both the wild-type and the FQ(I-391) mutant enzymes were fully oxidized (cf. also Figure 2B).

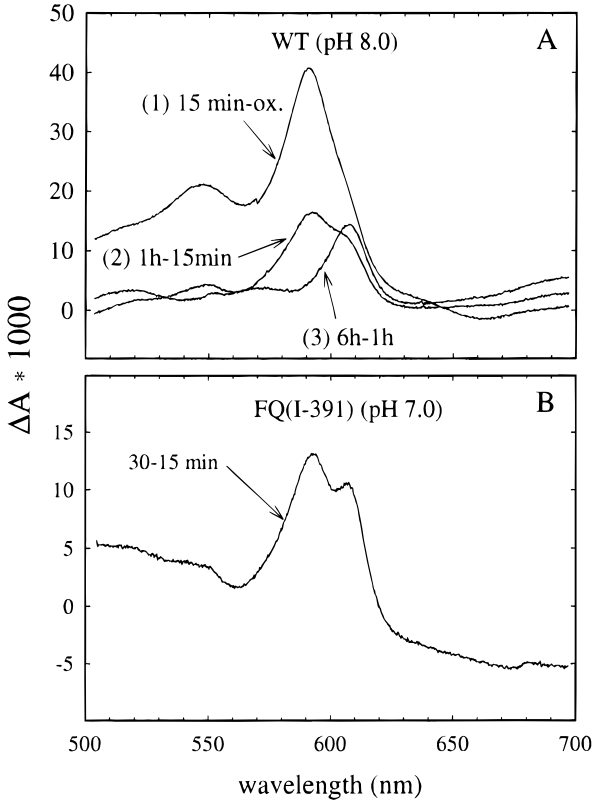

FIGURE 4: Difference spectra during incubation of the fully oxidized wild-type (at pH 8.0) (A) and FQ(I-391) mutant (at pH 7.0) (B) enzymes with CO. (A) Spectrum 1: difference of the spectra recorded 15 mim after and before addition of CO. The 590-nm peak is characteristic of the CO−heme a_3^{2+} species. Spectrum 2: Difference of the spectra recorded 1 h and 15 min after CO addition. The shoulder at 605 nm is indicative of fractional reduction of heme *a*. Spectrum 3: Difference of the spectra recorded 6 h and 1 h after CO addition. Only heme *a* was further reduced after one hour of CO incubation. (B) Difference of the spectra recorded 30 and 15 min after CO addition to the FQ(I-391) mutant enzyme. Immediately after CO addition a peak at 605 nm was observed. The peak at 590 nm developed during 15−30 min after CO addition and then the peak at 605 nm increased again. After 30 min of CO incubation (shown spectrum) the maximum a_3−CO relative to reduced heme *a* was observed. Different pHs were used for the wild-type and FQ(I-391) mutant enzymes because the heme *a*-reduction rate increases with increasing pH. At pH 7.0 heme *a* is reduced much slower than at pH 8.0 in the wild-type enzyme and at pH 7.0 essentially only an increase in absorbance at 590 nm is observed during the first hour of incubation. Conditions: 5 μM cytochrome *c* oxidase, 0.1% dodecyl β-D-maltoside, [CO] ≅ 1 mM, and 100 mM Hepes (at pH 7.0) or 100 mM Tris (at pH 8.0).

Electron-Transfer Reactions in Partly Reduced Enzyme. The partly reduced enzyme was prepared by incubation of the fully-oxidized enzyme under CO atmosphere (see Materials and Methods). In the wild-type enzyme this initially resulted in formation of the so-called mixed-valence state with oxidized heme a/Cu_A and reduced heme a_3/Cu_B with CO bound to heme a_3, characterized by an absorbance peak at 590 nm. Prolonged incubation resulted in a gradual reduction of heme *a*, forming the three-electron reduced enzyme, observed as an increase of the absorbance at 605 nm (Figure 4A). The reduction rate and the fraction three-electron reduced enzyme increased with increasing pH [cf. Brzezinski and Malmström (1985)], which is the reason why pH 8.0 was used with the wild-type enzyme. Figure 5A shows absorbance changes at 445 nm associated with electron transfer following dissociation of CO from the wild-type enzyme reduced to different degrees. In the mixed-valence

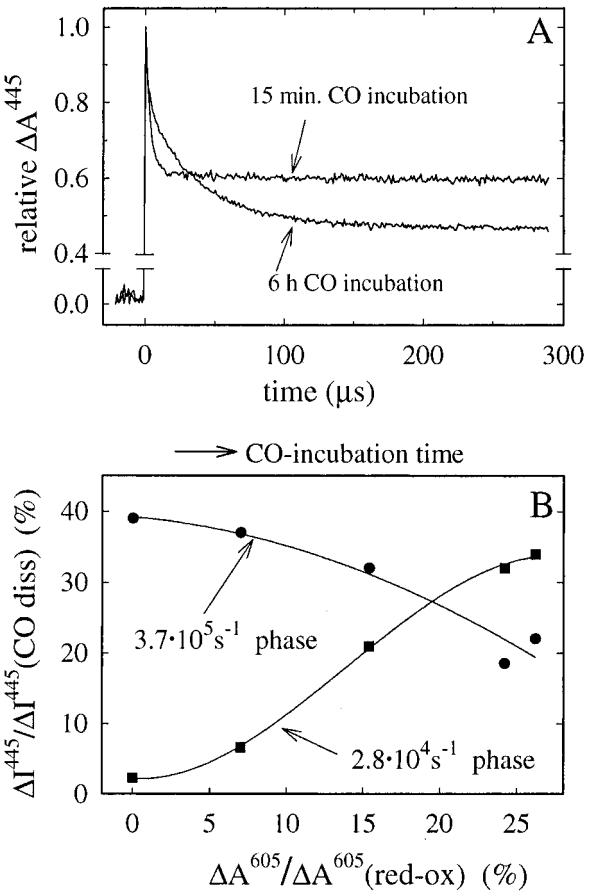

FIGURE 5: (A) Absorbance changes at 445 nm following flash photolysis of CO from wild-type cytochrome *c* oxidase reduced to different degrees. The oxidized enzyme was incubated under CO atmosphere for 15 min or 6 h. The traces are normalized to the CO dissociation absorbance changes. The faster (3.7×10^5 s^{-1}) and slower (2.8×10^4 s^{-1}) components correspond to electron transfer from heme a_3 to heme *a* and from hemes a/a_3 to Cu_A, respectively (there is also a contribution from CO recombination with a rate of about 50 s^{-1}). The CO ligand was flashed off at $t = 0$. The data shown are averages of five traces. (B) Relative amplitudes (intensities, *I*) of the faster and slower phases in A as a function of the reduction level of heme *a*. The kinetic-phase amplitudes are given in percent of the CO dissociation change. The reduction level of heme *a* is given as the ratio of the absorbance at 605 nm and the total reduced-minus-oxidized difference at 605 nm. The data corresponding to the point with the largest degree of reduction was collected after about 8 h of CO incubation. The enzyme was not reduced further after an additional 24 h incubation time. Conditions are the same as Figure 4, pH 8.0.

enzyme a rapid increase in absorbance, associated with CO dissociation was followed by a decrease in absorbance with an observed rate constant of 3.7×10^5 s^{-1}, associated with fractional electron transfer from heme a_3 to heme *a*, and a slower decrease in absorbance with a rate constant of 2.8×10^4 s^{-1}, associated with electron transfer from hemes a_3 and *a* to Cu_A. Further reduction of the two-electron reduced enzyme resulted in a decrease of the 3.7×10^5 s^{-1} phase amplitude and an increase of the 2.8×10^4 s^{-1} phase amplitude (Figure 5B), as has been observed previously in the mitochondrial enzyme (Morgan et al., 1989; Oliveberg & Malmström, 1991).

In the FQ(I-391) mutant oxidase heme *a* was reduced already after a short CO-incubation time (Figure 4B), even at relatively low pH. This is most likely a consequence of the higher redox potential of heme *a* relative to that of heme a_3 in the mutant compared to the wild-type enzyme.

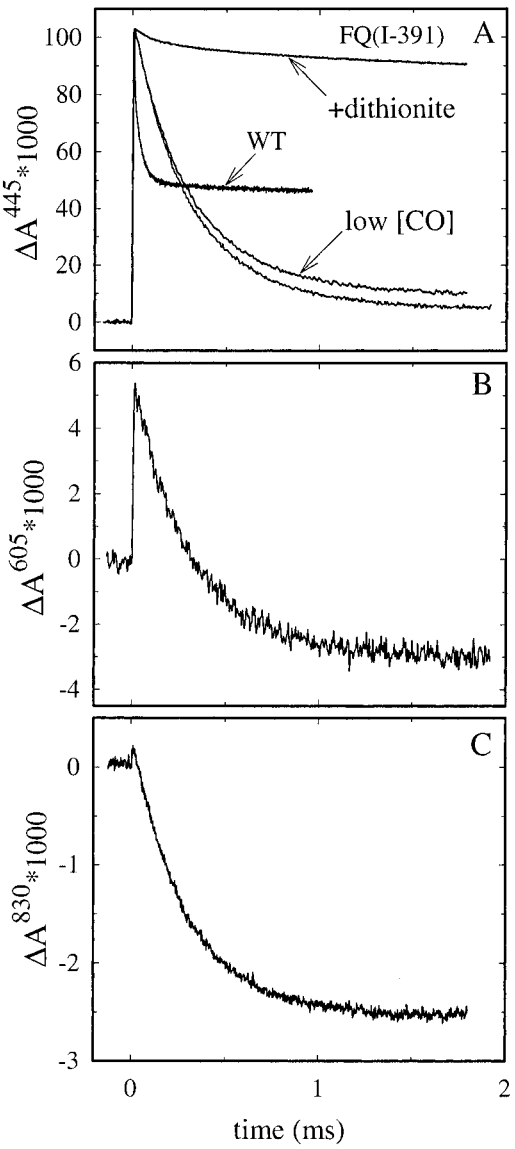

FIGURE 6: Absorbance changes after flash photolysis of CO from partly reduced FQ(I-391) mutant enzyme (except one trace in A, WT, which is the same trace as in Figure 5A after 15 min CO incubation) at 445 nm (A), 605 nm (B), and 830 nm (C). In panel (A) is also shown a trace recorded at low CO concentration (~0.1 mM). Absorbance changes in the fully-reduced enzyme (A) were recorded after addition of dithionite (~10 times molar excess). The CO ligand was flashed off at $t = 0$. The small rapid component at 445 nm after CO photolysis is probably due to a small fraction of the enzyme which is not fully reduced. Conditions: 1.5 μM cytochrome *c* oxidase, 100 mM Hepes, pH 8.0, 0.1% dodecyl β-D-maltoside, [CO] $\cong$ 1 mM (except for the low-[CO] trace in panel A).

Flash-induced absorbance changes associated with electron transfer following dissociation of carbon monoxide in the FQ(I-391) mutant enzyme were investigated at three different wavelengths: 445, 605, and 830 nm (Figure 6). At all three wavelengths the CO dissociation absorbance change was followed by a monoexponential decrease in absorbance with a rate constant of 3.2×10^3 s^{-1}. The absorbance changes at 445 and 605 nm were consistent with an ~80% oxidation of heme a_3, and the absorbance change at 830 nm was consistent with the same fraction reduced Cu_A. At 445 nm the rate constant of this phase did not change upon decrease of the CO partial pressure by a factor of ~10 (Figure 6A), which shows that the reaction associated with this absorbance change was independent of the CO-recombination rate. The

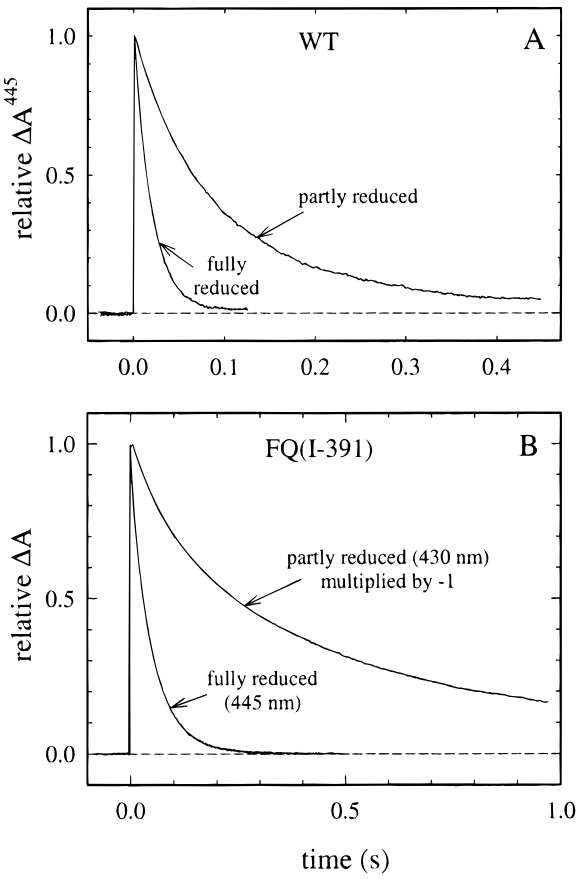

FIGURE 7: Absorbance changes associated with dissociation (at $t = 0$) and recombination of CO in partly- and fully-reduced wild-type (A) and FQ(I-391) mutant (B) enzymes. The FQ(I-391) partly-reduced trace was recorded at 430 nm because in the mutant enzyme at this wavelength the CO recombination absorbance change had a much larger contribution than at 445 nm, where electron transfer dominates (cf. Figure 6). For easier comparison, all traces were normalized and the 430 nm trace was multiplied by −1. Conditions were the same as in Figure 6.

3.2×10^3 s^{-1} absorbance change was not observed in the fully-reduced FQ(I-391) enzyme (Figure 6A).

Absorbance changes associated with CO recombination are shown in Figure 7. The rate constants[2] were 50 ± 5 and 15 ± 3 s^{-1} in the wild-type fully reduced and mixed-valence enzymes, respectively. In the FQ(I-391) mutant enzyme the corresponding rates were 25 ± 3 and 6 ± 1 s^{-1}, respectively. The relatively slower recombination rate in the partly-reduced FQ(I-391) mutant enzyme is consistent with the larger extent of electron transfer from heme a_3 because the observed recombination rate is determined by the fraction reduced heme a_3 times the recombination rate in the fully-reduced enzyme (Verkhovsky et al., 1992).

DISCUSSION

In this study we address the mechanisms of electron- and proton-transfer reactions in different states of cytochrome *c* oxidase. We have studied electron-transfer reactions in the presence and absence of O_2 in the wild-type and the Phe(I-391) → Gln (FQ(I-391)) mutant of cytochrome *c* oxidase from *R. sphaeroides*. In the mutant enzyme both rates and equilibrium constants are altered and we discuss these effects in terms of the functionality of the enzyme. The Phe(I-391) residue is highly conserved. The corresponding residue in the bovine enzyme (Phe(I-348)) is about 9 Å "below" the heme a_3 iron, 12 Å below Cu_B and 17 Å from the heme *a* iron (Tsukihara et al., 1995, 1996).

Electron-Transfer Reactions in Partly-Reduced Enzyme. In the wild-type two-electron reduced (mixed-valence) enzyme following CO dissociation there is first a rapid kinetic phase at 445 nm, associated with electron equilibration between hemes a_3 and *a* which results in an about 50% oxidation of heme a_3 (Ädelroth et al., 1995). The *forward* (heme *a* to a_3) rate constant was deconvoluted and was found to be $\sim 2 \times 10^5$ s^{-1}. The electron then equilibrates with Cu_A with a rate constant of 2.8×10^4 s^{-1}, observed as a second kinetic phase corresponding to at most 10% electron transfer to Cu_A.

Upon further reduction of the enzyme primarily heme *a* becomes reduced (Figure 4). As a result, following pulsed illumination, the amplitude of the rapid phase decreases whereas that of the slower phase increases (see Figure 5). In the three-electron reduced enzyme the kinetics become essentially monophasic and the absorbance changes correspond to oxidation of hemes *a* and a_3 and reduction of Cu_A [see also results from experiments on the bovine enzyme (Morgan et al., 1989)].

In the FQ(I-391) mutant oxidase only one kinetic phase, associated with electron transfer from heme a_3 to Cu_A, was observed following CO dissociation also from enzyme incubated a short time (∼15 min) under CO atmosphere. Since in the wild-type enzyme this is indicative of the three-electron reduced enzyme, one possibility to explain the different behavior of the mutant enzyme is that heme *a* becomes reduced in parallel with the binuclear center during incubation of the oxidized enzyme with CO and a dominating fraction of the partly-reduced FQ(I-391) enzyme is always three-electron reduced. This is supported by the presence of a peak at 605 nm in the optical difference absorption spectrum of the partly-reduced mutant enzyme already a short time after CO addition (Figure 4). In the mutant enzyme the heme *a* redox potential is higher and that of heme a_3 is presumably lower (see below) than in the wild-type enzyme. Therefore, it is likely that the three-electron reduced enzyme is formed more easily than in the wild-type enzyme. There is also a possibility that partly-reduced enzyme with hemes *a* and a_3 reduced and Cu_B oxidized is formed. However, this would not change the main conclusions of this work because Cu_B does not participate in the redox reactions after CO photolysis from the partly-reduced enzyme (the same fraction heme a_3 was oxidized as Cu_A reduced, see below).

From measurements at 445, 605, and 830 nm, we concluded that the extent of electron transfer from heme a_3 to Cu_A was ∼80%, which is significantly larger than in the wild-type enzyme even in the three-electron reduced state (Oliveberg et al., 1991). The redox titration shows that the redox potential of heme *a* is about 30 mV higher in the FQ-(I-391) mutant than in the wild-type enzyme. Consequently, to account for the larger extent of electron transfer either the redox potential of Cu_A must be higher or that of heme a_3 must be lower in the mutant than in the wild-type enzyme. It is unlikely that the Cu_A redox potential is affected because the mutation is far away from this site (Tsukihara, 1995, 1996; Iwata et al., 1995). We therefore assume that the heme

[2] In the partly-reduced enzymes the recombination kinetics were biphasic [see Ädelroth et al. (1995)]. The rate constants of the main components are given.

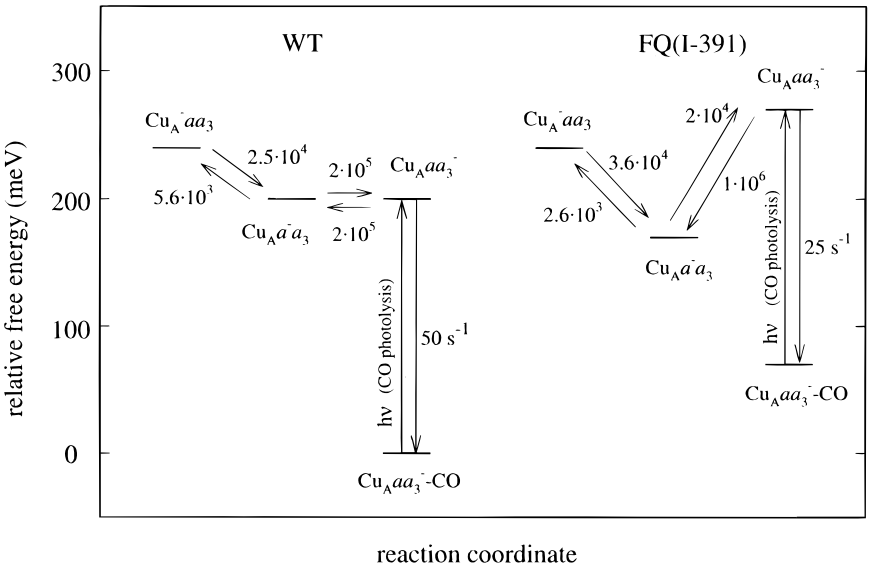

FIGURE 8: Electron-transfer reactions in partly-reduced wild-type and FQ(I-391) mutant cytochrome *c* oxidase in the absence of O_2. The energy levels and rate constants are calculated in Appendices 1 and 2. It is assumed that Cu_B stays reduced during the experiment (see text). Rate constants are given in s^{-1}.

a_3 redox potential is lower in the FQ(I-391) mutant than in the wild-type oxidase. The following scheme is used to model the electron transfer in the mutant enzyme:

$$Cu_A^- a^- a_3 \underset{k_{-1}^{FQ}}{\overset{k_1^{FQ}}{\rightleftharpoons}} Cu_A^- a a_3^- \underset{k_{-2}^{FQ}}{\overset{k_2^{FQ}}{\rightleftharpoons}} Cu_A a^- a^-{}_3 \qquad (1)$$

where a "−" sign symbolizes a reduced site and k_x are rate constants. The initial states immediately after CO dissociation are those with heme a_3 reduced. Using the above described assumptions and the model outlined in eq 1 we calculated the redox potential differences between the redox centers in the partly reduced enzymes from the extents of electron transfer in the wild-type and mutant enzymes (Appendix 1, Figure 8). In the mutant enzyme, in addition to the 30 mV higher redox potential of heme *a*, the redox potential of heme a_3 was estimated to be about 70 mV lower than in the wild-type enzyme. This corresponds to an about 50 times smaller equilibrium constant for electron transfer from heme *a* to a_3, i.e., $k_1^{FQ}/k_{-1}^{FQ} \cong 1/50$ as compared to ∼1 in the wild-type enzyme (Ädelroth et al., 1995).

In the FQ(I-391) mutant enzyme only one kinetic phase was observed. Consequently, all four rate constants in eq 1 could not be uniquely determined from a fit of the model to the experimental data. Since in the mutant enzyme $k_1^{FQ}/k_{-1}^{FQ} \cong 1/50$, i.e., $k_{-1}^{FQ} \gg k_1^{FQ}$ and in the wild-type enzyme $k_1^{WT} = k_{-1}^{WT} \cong 2 \times 10^5\ s^{-1}$ (Ädelroth et al., 1995), it is likely that k_{-1}^{FQ} is at least $2 \times 10^5\ s^{-1}$ (if $k_{-1}^{FQ} = 2 \times 10^5\ s^{-1}$, $k_1^{FQ} = 4 \times 10^3\ s^{-1}$, see Figure 8). Using this assumption, a fit of the model to the experimental data gives $k_2 = 3.6 \times 10^4\ s^{-1}$ and $k_{-2} = 2.6 \times 10^3\ s^{-1}$ (Appendix 2). Note that these values of k_2 and k_{-2} are obtained for any $k_{-1}^{FQ} \gg k_1^{FQ}$, k_{-2}^{FQ}, k_2^{FQ}.

It is interesting to note that an increase of the driving force for electron transfer from Cu_A to heme *a* by ∼30 meV results in an increased electron-transfer rate ($3.6 \times 10^4\ s^{-1}$ in FQ(I-391) and $2.5 \times 10^4\ s^{-1}$ in WT, Appendix 2), which is consistent with a Marcus equation [for a review see Marcus and Sutin (1985)] based model (Brzezinski, 1996).

Values of k_1^{FQ} and k_{-1}^{FQ} were estimated from the driving-force dependencies ($-\Delta G$) of these rate constants in the wild-type enzyme using a model discussed recently (Brzezinski, 1996). Assuming the same electron-transfer distance and reorganization energy in the wild-type and FQ(I-391) mutant enzymes, for a driving force about 100 mV smaller than in the wild-type enzyme we obtain $k_1^{FQ} \cong 2 \times 10^4\ s^{-1}$ and $k_{-1}^{FQ} \cong 1 \times 10^6\ s^{-1}$.

The rates and equilibrium constants in the wild-type and FQ(I-391) enzymes discussed above are summarized in the energy diagram in Figure 8.

Reaction of the Fully-Reduced Enzyme with O_2. After photolysis of CO from the fully-reduced enzyme in the presence of ∼1 mM dioxygen (flow−flash method) in the wild-type enzyme three major kinetic phases were observed in the Soret region with rate constants of 4×10^4, 8×10^3, and $6 \times 10^2\ s^{-1}$, respectively. The same method in combination with various spectroscopic techniques has been used extensively to investigate the reaction of the mitochondrial fully reduced enzyme with O_2 (see introduction). In this enzyme O_2 binding to heme a_3 with a rate of about $10^5\ s^{-1}$ is followed by three kinetic phases at 445 nm with rate constants of $3 \times 10^4\ s^{-1}$ ($\Delta A^{445} < 0$), $1 \times 10^4\ s^{-1}$ ($\Delta A^{445} > 0$), and $1 \times 10^3\ s^{-1}$ ($\Delta A^{445} < 0$), respectively (at ∼1 mM O_2, see introduction). The first phase is an absorbance decrease which is associated with electron transfer from heme *a* to the binuclear center and formation of the peroxy intermediate (P). This is then followed by an increase in absorbance associated with fractional electron transfer from Cu_A to heme *a* and concomitant formation of the ferryl intermediate (F). The slowest phase corresponds to transfer of the fourth electron to the binuclear center from Cu_A/heme *a* forming the fully-oxidized enzyme (O). The bacterial wild-type enzyme displayed the same type of kinetic characteristics even though the intermediate phase was not observed at 445 nm because its amplitude is smaller than in the bovine enzyme (it is observed, e.g., at 430 nm and in the α region; Ädelroth et al., unpublished). In the FQ(I-391) mutant enzyme the first kinetic phase had a rate of $1.2 \times 10^5\ s^{-1}$. Its kinetic difference spectrum (Figure 3) was similar to that of the heme a_3 ferrous−oxy intermediate observed in the bovine enzyme (Verkhovsky et al., 1994), which indicates

that O_2 is bound to the same extent in the FQ(I-391) mutant enzyme as in the bovine enzyme. In the wild-type enzyme the O_2 binding is followed and obscured by oxidation of hemes *a* and a_3 concomitant with formation of the P intermediate. Heme *a* oxidation was much slower (30 s^{-1}) in the mutant enzyme and the P intermediate was most likely formed with electrons from heme a_3 and Cu_B. This is similar to the situation observed in the mixed-valence bovine enzyme where a stable P intermediate is formed with a rate of about 6×10^3 s^{-1} (Hill & Greenwood, 1983; Oliveberg et al., 1989). In other words the difference between the mechanisms of P-intermediate formation in the wild-type and FQ-(I-391) mutant enzymes is the source from which the second electron is taken (heme *a* or Cu_B).

In the mutant enzyme the electron-transfer rate from heme *a* to heme a_3 is presumably reduced by only a factor of 10 (even if k_{-1}^{FQ} would have the same value as in the wild-type enzyme (2×10^5 s^{-1}), the forward rate, k_1^{FQ}, would be 4×10^3 s^{-1}), which cannot alone account for the dramatically slowed electron-transfer rate from heme *a* during oxygen reduction. Therefore, most likely the slower oxidation rate of heme *a* is also due to the 100 meV smaller driving force for the electron transfer from heme *a* to heme a_3.

The mechanism of the P-intermediate formation in the fully-reduced enzyme has been discussed by Verkhovsky et al. (1994) who suggested that during the early steps of O_2 reduction the different intermediates up to P are at equilibrium and that the P state is unfavorable until it is stabilized by transfer of the third electron to the binuclear center. The model cannot fully explain the results obtained with the FQ(I-391) mutant enzyme because after P(Fe_a^{2+}) is formed (P with electrons from the binuclear center, heme *a* remains reduced) with a rate of about 4×10^3 s^{-1}, electron transfer from heme *a* to the binuclear center (forming P(Fe_a^{3+})) should procede with a (faster) rate of about 2×10^4 s^{-1} (i.e., the intrinsic electron-transfer rate, see Figure 8). Consequently, the apparent rate of P(Fe_a^{3+}) formation would be about 4×10^3 s^{-1}.

During oxidation of the bovine fully-reduced enzyme the A → P(Fe_a^{3+}) transition (3×10^4 s^{-1} phase, formation of the P intermediate with electrons from hemes *a* and a_3) has been suggested to be coupled to an internal proton transfer stabilizing the P(Fe_a^{3+}) intermediate (Hallén & Nilsson 1992). Hence, it is likely that an internal proton-transfer reaction (e.g., to a group nearby the binuclear center) is rate limiting for formation of the P intermediate. In the fully-reduced wild-type enzyme this is followed by electron transfer from heme *a* to the binuclear center with a rate constant larger than 3×10^4 s^{-1} and P(Fe_a^{3+}) with only two electrons at the binuclear center is not detected. In the FQ(I-391) mutant enzyme a stable P(Fe_a^{2+}) intermediate with both electrons from the binuclear center is found because the electron equilibrium is shifted away from the binuclear center and electron transfer from heme *a*/Cu_A (oxidation of the enzyme) is driven by the following reaction steps (P(Fe_a^{2+}) → P(Fe_a^{3+}) → F → O) (Figure 9), which is a slow process because the fraction P(Fe_a^{3+}) is very small. In other words, the apparent rate of the reaction (30 s^{-1}) is determined by the fraction P(Fe_a^{3+}) formed and the rate of the following step(s). From this follows that in the FQ(I-391) mutant enzyme the driving force for electron transfer from heme *a* to the binuclear center in the P(Fe_a^{2+}) state must be ≤ −60 meV (i.e., $\Delta G \geq 60$ meV) because no electron transfer is detected (assuming a 10% detection limit for electron transfer from heme *a*). Assuming that the driving force for electron transfer from heme *a* to the binuclear center is 100 meV smaller in the FQ(I-391) mutant than in the wild-type enzyme (see above) the driving force in the wild-type enzyme must be ≤40 meV. It should not be smaller than about 30 meV because substantial electron transfer from heme *a* to the binuclear center is observed in the wild-type enzyme (30 meV corresponds to about 75% electron transfer). The relatively small loss of energy up to formation of the P(Fe_a^{3+}) intermediate with three electrons at the binuclear center is consistent with the observation that this state can be photolyzed to regenerate the fully-reduced state (Varotsis & Babcock, 1995).

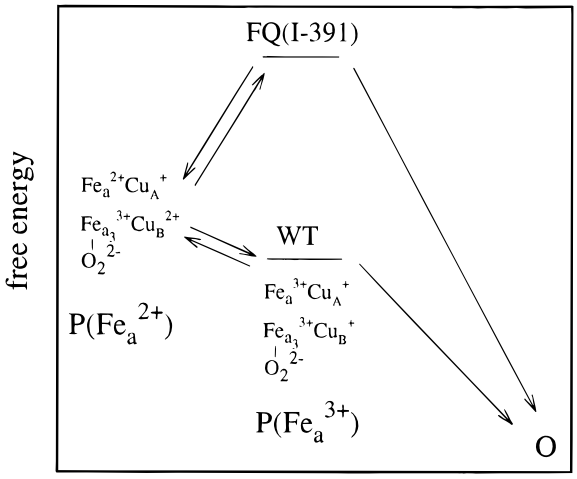

FIGURE 9: Model for the reactions following formation of the P intermediate in the FQ(I-391) mutant and wild-type enzymes. The P intermediate is formed with electrons from hemes *a* and a_3 (P(Fe_a^{3+})) or from the binuclear center (P(Fe_a^{2+})) with rates of 40 000 and 4000 s^{-1}, respectively. In the FQ(I-391) mutant enzyme the altered redox potential difference between the hemes makes electron transfer from heme *a* unfavorable in the state P(Fe_a^{2+}) and the concentration of P(Fe_a^{3+}) is small; the overall reaction is driven by the following steps, i.e., the P(Fe_a^{3+}) → F → O transitions [only the P(Fe_a^{3+}) → O step is shown]. The apparent rate is slow (30 s^{-1}) because the fraction P(Fe_a^{3+}) is small. Proton uptake is not shown explicitly.

It is interesting to note that the rate of the slowest phase during oxidation of the fully-reduced enzyme is about the same as the overall turnover rate, which indicates that the lower activity of the mutant enzyme is due to inhibition of electron transfer from heme *a*/Cu_A to the binuclear center.

CONCLUSIONS

The results from this work show that the reduced overall activity of the FQ(I-391) mutant enzyme is due to slower electron transfer from heme *a* (and Cu_A) to the binuclear center during O_2 reduction. In addition, the results indicate that there is a direct relation between the redox potential difference between hemes *a* and a_3 (as determined from redox titrations and studies of electron-transfer reactions in the partly-reduced enzyme) and the kinetics of electron transfer to the binuclear center during O_2 reduction.

APPENDICES

Results from the calculations in Appendices 1 and 2 are summarized in Figure 8.

Appendix 1. Redox Potential Differences between the Redox Centers

Two-Electron Reduced Wild-Type Enzyme

The following model is used (Cu_B is omitted for clarity):

$$Cu_A^- a a_3 \overset{K_2/\Delta E_2}{\rightleftharpoons} Cu_A a^- a_3 \overset{K_1/\Delta E_1}{\rightleftharpoons} Cu_A a a_3^- \qquad (2)$$

where K_1 and K_2 are equilibrium constants and $\Delta E_1 = E_{a_3} - E_a$ and $\Delta E_2 = E_a - E_{Cu_A}$ are the redox potential differences between the redox sites indicated by the indexes. Before CO photolysis only state $Cu_A a\, a_3^-$ is populated because CO stabilizes the electron at heme a_3. After CO photolysis an equilibrium is established between all three states. The fractions reduced Cu_A, heme *a*, and heme a_3 are

$$[Cu_A^-] = (1 + K_2 + K_1K_2)^{-1} \qquad (3)$$

$$[a^-] = K_2\,(1 + K_2 + K_1K_2)^{-1} \qquad (4)$$

$$[a_3^-] = K_1K_2\,(1 + K_2 + K_1K_2)^{-1} \qquad (5)$$

$$K_1 = \exp\left(\frac{E_{a_3} - E_a}{RT/F}\right) \qquad (6)$$

$$K_2 = \exp\left(\frac{E_a - E_{Cu_A}}{RT/F}\right) \qquad (7)$$

In the wild-type enzyme we use $E_{a_3}^{WT} - E_a^{WT} = 0$ (Ädelroth et al., 1995), i.e., $K_1^{WT} = 1$ and the degree of reduction of Cu_A in the wild-type enzyme, $[Cu_A^-]^{WT}$, is ~0.1, which together with eq 3 gives

$$K_2^{WT} = \frac{1 - [Cu_A^-]^{WT}}{[Cu_A^-]^{WT}\,(1 + K_1^{WT})} \cong 4.5 \qquad (8)$$

From eq 7 we obtain $E_a^{WT} - E_{Cu_A}^{WT} \cong 40$ mV.

Three-Electron Reduced FQ(I-391) Mutant Enzyme

As discussed in the discussion section the partly reduced FQ(I-391) mutant enzyme accommodates three electrons, i.e., an additional electron is found at heme *a*/Cu_A:

$$Cu_A^- a^- a_3 \overset{K_1/E_1}{\rightleftharpoons} Cu_A^- a a_3^- \overset{K_2/E_2}{\rightleftharpoons} Cu_A a^- a^-{}_3 \qquad (9)$$

The redox potential of heme *a* in the FQ(I-391) mutant enzyme is about 30 mV higher than that in the wild-type enzyme, whereas that of Cu_A is the same (see Discussion):

$$E_a^{FQ} = E_a^{WT} + \delta E_a \qquad (10)$$

Equations 7 and 10 together with $K_2^{WT} \cong 4.5$ (eq 8) and $\delta E_a = 30$ mV give

$$K_2^{FQ} = \exp\left(\frac{E_a^{FQ} - E_{Cu_A}}{RT/F}\right) = \exp\left(\frac{E_a^{WT} - E_{Cu_A}}{RT/F}\right)\exp\left(\frac{\Delta E_a}{RT/F}\right) = K_2^{WT}\exp\left(\frac{\delta E_a}{RT/F}\right) \cong 14 \qquad (11)$$

Before CO photolysis the electron is stabilized on reduced heme a_3 (states $Cu_A^- a a_3^-$ and $Cu_A a^- a_3^-$). Since $K_2^{FQ} \cong 14$ the population of state $Cu_A^- a a_3^-$ is only about 6%. Therefore, we assume that state $Cu_A a^- a_3^-$ is the initial state prior to CO photolysis, i.e., the reduction level of Cu_A is ~0 prior to CO dissociation.

The reduction level of Cu_A after CO dissociation is

$$[Cu_A^-]^{FQ} = \frac{1 + K_1^{FQ}}{1 + K_1^{FQ} + K_1^{FQ}K_2^{FQ}} \qquad (12)$$

K_1^{FQ} is calculated using eq 12 with $K_2^{FQ} \cong 14$ and $[Cu_A^-]^{FQ} = 0.8$ as

$$K_1^{FQ} = \frac{1 - [Cu_A^-]^{FQ}}{[Cu_A^-]^{FQ}(1 + K_2^{FQ}) - 1} = 0.018 \qquad (13)$$

which gives

$$E_{a_3}^{FQ} - E_a^{FQ} \cong -100 \text{ mV}$$

Thus, in the FQ(I-391) mutant oxidase the redox potential of heme *a* is 30 mV higher than in the wild-type enzyme and that of heme a_3 is 70 mV lower.

Appendix 2. Kinetics

The following general model will be used for both the two-electron reduced wild-type and the three-electron reduced FQ(I-391) mutant enzymes:

$$A \underset{k_{-i}}{\overset{k_i}{\rightleftharpoons}} B \underset{k_{-ii}}{\overset{k_{ii}}{\rightleftharpoons}} C, \qquad [C](t{=}0) = 1 \qquad (14)$$

$$[A] = k_{-i}k_{-ii}\left(\frac{1}{\kappa_1\kappa_2} + \frac{1}{\kappa_1(\kappa_1 - \kappa_2)}e^{-\kappa_1 t} + \frac{1}{\kappa_2(\kappa_2 - \kappa_1)}e^{-\kappa_2 t}\right) \qquad (15)$$

$$[B] = k_{-ii}\left(\frac{k_i}{\kappa_1\kappa_2} + \frac{k_i - \kappa_1}{\kappa_1(\kappa_1 - \kappa_2)}e^{-\kappa_1 t} + \frac{k_i - \kappa_2}{\kappa_2(\kappa_2 - \kappa_1)}e^{-\kappa_2 t}\right) \qquad (16)$$

$$[C] = 1 - ([A] + [B]) \qquad (17)$$

where

$$\kappa_{1,2} = \frac{(k_i + k_{ii} + k_{-i} + k_{-ii})}{2} \pm \sqrt{\frac{(k_i + k_{ii} + k_{-i} - k_{-ii})^2}{4} - k_ik_{ii} - k_ik_{-ii} - k_{-i}k_{-ii}} \qquad (18)$$

Two-Electron Reduced Wild-Type Enzyme

To begin, $k_i \equiv k_2^{WT}$; $k_{-i} \equiv k_{-2}^{WT}$; $k_{ii} \equiv k_1^{WT}$; and $k_{-ii} \equiv k_{-1}^{WT}$.

$$Cu_A^- a a_3 \overset{k_2^{WT}}{\underset{k_{-2}^{WT}}{\rightleftharpoons}} Cu_A a^- a_3 \overset{k_1^{WT}}{\underset{k_{-1}^{WT}}{\rightleftharpoons}} Cu_A a a^-{}_3 \qquad (19)$$

The equilibrium constants $K_1^{WT} = k_1^{WT}/k_{-}^{WT}{}_1$ and $K_2^{WT} = k_2^{WT}/k_{-2}^{WT}$ are 1 and 4.5, respectively (see Appendix 1) and thus $k_1^{WT} = k_{-1}^{WT}$. In addition, k_1^{WT}, $k_{-1}^{WT} \gg k_2^{WT}$, k_{-2}^{WT} (see Results). Equation 18 then simplifies to

$$\kappa_{1,2} \cong k_1\left(1 \pm \sqrt{1 - \frac{2k_2 + k_{-2}}{k_1}}\right) \cong k_1\left(1 \pm \left(1 - {}^1/_2\,\frac{2k_2 + k_{-2}}{k_1}\right)\right) \quad (20)$$

$$\kappa_1 \cong 2k_1,\ \kappa_2 \cong {}^1/_2(2k_2 + k_{-2}) \quad (21)$$

(Indexes "WT" are omitted for clarity.)

The observed rate constants are 3×10^5 and 2.8×10^4 s^{-1}, which gives $k_1 = k_{-1} = 1.5 \times 10^5$ s^{-1} and $k_2 = 25\,000$ s^{-1}, $k_{-2} = 5600$ s^{-1}.

Three-Electron Reduced FQ(I-391) Mutant Enzyme

To begin, $k_i \equiv k_1^{FQ}$; $k_{-i} \equiv k_{-1}^{FQ}$; $k_{ii} \equiv k_2^{FQ}$; and $k_{-ii} \equiv k_{-2}^{FQ}$.

$$Cu_A^- a^- a_3 \underset{k_{-1}^{FQ}}{\overset{k_1^{FQ}}{\rightleftharpoons}} Cu_A^- a a_3^- \underset{k_{-2}^{FQ}}{\overset{k_2^{FQ}}{\rightleftharpoons}} Cu_A a^- a^-{}_3 \quad (22)$$

$K_1^{FQ} = k_1^{FQ}/k_{-1}^{FQ}$ and $K_2^{FQ} = k_2^{FQ}/k_{-2}^{FQ}$ are 0.018 and 14, respectively (see Appendix 1), and $k_{-1}^{FQ} \gg k_1^{FQ}, k_2^{FQ}, k_{-2}^{FQ}$ (see Discussion). Equation 18 then simplifies to

$$\kappa_{1,2} \cong \frac{k_{-2}}{2}\left(1 \pm \sqrt{1 - 4\frac{k_1k_2 + k_{-1}k_{-2}}{k_{-1}^2}}\right) \cong \frac{k_{-1}}{2}\left(1 \pm \left(1 - 2\,\frac{k_1k_2 + k_{-1}k_{-2}}{k_{-1}^2}\right)\right) \quad (23)$$

(Indexes "FQ" are omitted for clarity.)

$$\kappa_1^{FQ} \cong k_{-1}^{FQ},\ k_2^{FQ} \cong \frac{k_1^{FQ}\,k_2^{FQ}}{k_{-1}^{FQ}} + k_{-2}^{FQ} = K_1^{FQ}\,k_2^{FQ} + k_{-2}^{FQ} \quad (24)$$

The value of k_{-1}^{FQ} was estimated to be about 10^6 s^{-1} (see Discussion). Since $k_{-1}^{FQ} \gg k_1^{FQ}, k_2^{FQ}, k_{-2}^{FQ}$ and thus $\kappa_1^{FQ} \gg \kappa_2^{FQ}$ the concentration of [B] (eq 14) is ~0 during the course of the reaction. State C disappears with the rate constant κ_2^{FQ} and state A is formed with the same rate. The observed reaction rate, i.e., κ_2^{FQ}, is 3200 s^{-1}. Using eq 24, $k_2^{FQ} \cong 36\,000$ s^{-1} and $k_{-2}^{FQ} \cong 2600$ s^{-1}.

REFERENCES

Ädelroth, P., Brzezinski, P., & Malmström B. G. (1995) *Biochemistry 34*, 2844−2849.

Ädelroth, P., Sigurdson, H., Hallén, S., & Brzezinski P. (1996) *Proc. Natl. Acad. Sci. U.S.A. 93*, 12292−12297.

Antalis, T. M., & Palmer, G. (1982) *J. Biol. Chem. 257*, 6194−6206.

Babcock, G. T., & Wikström, M. (1992) *Nature 356*, 301−309.

Babcock, G. T., & Varotsis, C. (1993) *J. Bioenerg. Biomembr. 25*, 71−80.

Boelens R., Wever R., & Van Gelder, B. F. (1982) *Biochim. Biophys. Acta 682*, 264−272.

Brzezinski, P. (1996) *Biochemistry 35*, 5611−5615.

Brzezinski, P., & Malmström, B. G. (1985) *FEBS Lett. 187*, 111−114.

Brzezinski, P., & Malmström, B. G. (1987) *Biochim. Biophys. Acta 894*, 29−38.

Calhoun, M. W., Thomas, J. W., & Gennis, R. B. (1994) *Trends Biochem. Sci. 19*, 325−330.

Ferguson-Miller, S., & Babcock, G. T. (1996) *Chem. Rev. 96*, 2889−2907.

Gibson, Q. H., & Greenwood, C. (1963) *Biochem. J. 86*, 541−554.

Hallén, S., & Nilsson, T. (1992) *Biochemistry 31*, 11853−11859.

Hallén, S., & Brzezinski, P. (1994) *Biochim. Biophys. Acta 1184*, 207−218.

Han, S., Ching, Y.-C., & Rousseau, D. L. (1990a) *Proc. Natl. Acad. Sci. U.S.A. 87*, 2491−2495.

Han, S., Ching, Y.-C., & Rousseau, D. L. (1990b) *Proc. Natl. Acad. Sci. U.S.A. 87*, 8408−8412.

Hill, B. C. (1991) *J. Biol. Chem. 266*, 2219−2226.

Hill, B. C., & Greenwood, C. (1983) *Biochem J. 215*, 659−667.

Hill, B. C., & Greenwood, C. (1984) *Biochem J. 218*, 913−921.

Hosler J. P., Fetter J., Tecklenburg M. M. J., Espe M. Lerma C., & Ferguson-Miller, S. (1992) *J. Biol. Chem. 267*, 24264−24272.

Iwata, S., Ostermeier, C., Ludwig, B., & Michel, H. (1995) *Nature 376*, 660−669.

Marcus, R. A., & Sutin, N. (1985) *Biochim. Biophys. Acta 811*, 265−322.

Mitchell, D. M. (1996) Ph.D. Thesis, University of Illinois at Urbana−Champaign.

Mitchell, D. M., & Gennis, R. B. (1995) *FEBS Lett. 368*, 148−150.

Morgan, J. E., Li, P. M., Jang, D.-J., El-Sayed, M. A., & Chan, S. I. (1989) *Biochemistry 28*, 6975−6983.

Morgan, J. E., Verkhovsky, M. I., & Wikström, M. (1996) *Biochemistry 35*, 12235−12240.

Ogura, T., Takahashi, S., Shinzawa-Itoh, K., Yoshikawa, S., & Kitagawa, T. (1990) *J. Am. Chem. Soc. 112*, 5630−5631.

Oliveberg, M., & Malmström, B. G. (1991) *Biochemistry 30*, 7053−7057.

Oliveberg, M., Brzezinski, P., & Malmström, B. G. (1989) *Biochim. Biophys. Acta 977*, 322−328.

Sarti, P., Antonini, G., Malatesta, F., Vallone, B., & Brunori, M. (1990) *Ann. N.Y. Acad. Sci. 550*, 161−166.

Sucheta, A., Georgiadis, K. E., & Einarsdóttir, Ó (1997) *Biochemistry 36*, 554−565.

Svensson Ek, M., & Brzezinski, P. (1997) *Biochemistry 36*, 5425−5431.

Tsukihara, T., Aoyama, H., Yamashita, E., Tomizaki, T., Yamaguchi, H., Shinzava-Itoh, K., Nakashima, R., Yaono, R., & Yoshikawa, S. (1995) *Science 269*, 1069−1074.

Tsukihara, T., Aoyama, H., Yamashita, E., Tomizaki, T., Yamaguchi, H., Shinzava-Itoh, K., Nakashima, R., Yaono, R., & Yoshikawa, S. (1996) *Science 272*, 1136−1144.

Varotsis, C. A., & Babcock, G. T. (1995) *J. Am. Chem. Soc. 117*, 11260−11269.

Varotsis, C., Woodruff, W. H., & Babcock, G. T. (1989) *J. Am. Chem. Soc. 111*, 6439−6440.

Verkhovsky, M. I., Morgan, J. E., & Wikström, M. (1992) *Biochemistry 31*, 11860−11863.

Verkhovsky M. I., Morgan, J. E., & Wikström, M. (1994) *Biochemistry 33*, 3079−3086.

BI962824S